jmr&t
Journal of Materials Research and Technology
www.jmrt.com.br

Original Article

# An analytical model of heat generation for eccentric cylindrical pin in friction stir welding

*Ahmed Ramadan Shaaban Essa*[a,*], *Mohamed Mohamed Zaky Ahmed*[b], *Abdel-Karim Yousif Ahmed Mohamed*[a], *Ahmed Essa El-Nikhaily*[a]

[a] *Department of Mechanical, Faculty of Industrial Education, Suez University, Suez, Egypt*
[b] *Department of Metallurgical and Materials Engineering, Faculty of Petroleum and Mining Engineering, Suez University, Suez, Egypt*

ARTICLE INFO

*Article history:*
Received 14 July 2015
Accepted 12 November 2015
Available online 20 January 2016

*Keywords:*
Friction stir welding
Analytical modeling
Pin eccentricity

ABSTRACT

An analytical model for heat generation for eccentric cylindrical pin in friction stir welding was developed that utilizes a new factor based on the tool pin eccentricity. The proposed analytical expression is a modification of previous analytical models from the literature, which is verified and well matches with the model developed by previous researchers. Results of plunge force and peak temperature were used to validate the current proposed model. The cylindrical tool pin with eccentricities of 0, 0.2, and 0.8 mm were used to weld two types of aluminum alloys; a low deformation resistant AA1050-H12, and a relatively high deformation resistant AA5754-H24 alloy. The FSW was performed at constant tool rotation speed of 600 rpm and different welding speeds of 100, 300, and 500 mm/min. Experimental results implied that less temperature is generated using eccentric cylindrical pin than cylindrical pin without eccentricity under the given set of FSW process conditions. Furthermore, numerical simulation results show that increasing the pin eccentricity leads to decrease in peak temperature.



## 1. Introduction

Friction stir welding tool plays the main role in the solid state welding process and is being developed up to date to enhance the weld quality and process efficiency. In friction stir welding (FSW) a non-consumable, cylindrical, and shouldered tool with a profiled probe is rotated and slowly plunged into the joint line between two pieces of sheet or plate material, which are butted together [1]. The parts have to be clamped onto a backing bar in a manner that prevents the abutting joint faces from being forced apart. Frictional heat is generated between the wear resistant welding tool and the material of the work piece [2]. This heat causes the latter to soften without reaching the melting point and allows the tool to traverse along the weld line [3]. The plasticized material is transferred from the tool leading edge (advancing side) to its trailing edge (retreating side) and is forged by the intimate contact of the tool

* *Corresponding author.*
E-mail: ahmed.eessa@suezuniv.edu.eg (A.R.S. Essa).
http://dx.doi.org/10.1016/j.jmrt.2015.11.009

**Nomenclature**

| | |
|---|---|
| $Q$ | heat generation (W) |
| $Q_1$ | heat generation from shoulder (W) |
| $Q_2$ | heat generation from pin side (W) |
| $Q_3$ | heat generation pin tip (W) |
| $Q_{Total}$ | total heat generation (W) |
| $R_p$ | pin radius (mm) |
| $R_s$ | shoulder radius (mm) |
| $H_p$ | pin height (mm) |
| $e$ | pin eccentricity (mm) |
| $\mu$ | friction coefficient |
| $\omega$ | tool angular speed (rad/s) |
| $\alpha$ | shoulder concave angle (°) |
| $\upsilon$ | welding speed (m/s) |
| $p$ | contact pressure (Pa) |
| $\tau_{contact}$ | contact shear stress (Pa) |
| $T_{max}$ | maximum welding temperature (°C) |
| $T_s$ | solidus temperature (°C) |

shoulder and the pin profile, and leaves a solid phase bond between the two pieces [4–6]. Since 1991, the tool geometry has evolved appreciably and the tool material properties have become better and better. However, the evolution is not ended; further improvements are needed in this field. There is a growing demand of welding high melting temperature, and high strength, as well as hardened materials. The key issues are the tool design and the tool material itself [7]. The rotation and movement of the tool through the workpiece may cause the tool to get worn and it may also deform plastically at elevated temperatures [8]. Friction stir welding of hard alloys is limited today by the high cost and short life of tools [8]. The effect of tool shape on friction stir welding has not yet been systematically explored. The tool shape should be as simple as possible to reduce the cost, and the stirring effect should be sufficient to produce sound joints [9].

The primary function of the rotating tool pin is to stir the plasticized metal and move it from front to the back of the pin to have good joint [10]. Elangovan et al. [11] studied the influences of tool pin profile and tool shoulder diameter on the formation of friction stir processing zone, and reported that the pin profile plays a crucial role in material flow. Accordingly, it regulates the welding speed of the FSW process. The pin is generally cylindrical, frustum tapered, threaded or flat. Pin profiles with flat faces (square or triangular) are sometime associated with eccentricity, which allows incompressible material to pass around the pin profile.

Thomas and Nicholas [12] reported that the tool pin eccentricity is associated with a dynamic orbit, which becomes part of the FSW process. Furthermore, research modern trends involve the effect of tool eccentricity in friction stir welding [13,14]. Recently, the effect of tool pin eccentricity on microstructure and mechanical properties in friction stir welded 7075 aluminum alloy thick plate has been investigated, using a tapered threaded pin. It has been found that, the highest mechanical properties of FSW joints were those produced using 0.2 mm pin eccentricity [15].

Modeling of FSW for heat generation was presented by number of studies [16–18]. Khandkar et al. [16] introduced a torque based heat input model for straight cylindrical pin profile. Schmidt et al. [17] developed an analytical model for heat generation for straight cylindrical pin profile having concave shoulder in FSW based on different assumptions in terms of contact condition between the rotating tool surface and the weld piece. Furthermore, Gadakh et al. [18] developed an analytical model for heat generation for tapered cylindrical pin profile having flat shoulder in FSW based on different assumptions in terms of contact condition.

Nowadays, the analytical models developed are only for cylindrical pin without eccentricity [17,18]. It has been reported [15] that the use of FSW tool with pin eccentricity resulted in better mechanical properties than that obtained using FSW tool pin without eccentricity [15]. Thus, there is a need for developing an analytical model for heat generation during the use of eccentric cylindrical pin in FSW that is developed in this paper.

The proposed analytical expression is a modification of previous analytical models developed by Schmidt et al. [17] and Gadakh et al. [18].

The model aims to estimating the heat generated for tool with pin eccentricity in FSW. This generated energy and the associated maximum temperature are compared to the results measured in experimental work to verify the proposed model.

## 2. Experimental procedure

The FSW tools used for welding were cut from 40 mm diameter H13 cold worked tool steel rod (0.39% C, 0.1% Si, 0.40% Mn, 5.2% Cr, 0.95% V, 1.4% Mo, and 90.6 wt% Fe), and heat-treated to 62 HRC. Tools with three different designs were prepared. The first, was with a cylindrical tool pin without eccentricity, in which the pin and shoulder axes are aligned. The second was also with a cylindrical pin but with 0.2 mm eccentricity, i.e. the pin axis is shifted by 0.2 mm from the tool axis. The third tool was with a cylindrical pin with eccentricity of 0.8 mm. In all cases, the smooth 19 mm diameter shoulder is with 2° concavity, and the pin length was 4.6 mm with 6 mm diameter.

Friction stir welding of butt joints of AA1050-H12, and AA5754-H24 aluminum alloys was performed using FSW machine of 22 kW power with max rotation speed of 3000 rpm, max welding speed of 1000 mm/min, and max vertical force of 100 kN. The chemical composition of the studied alloys are listed in Table 1.

The solidus temperature ($T_s$) for AA1050-H12, and AA5754-H24 aluminum alloys according to ASM are 646 °C and 583 °C, respectively. The weld samples were made of two plates of 5 mm thick, 100 mm wide, and 200 mm length.

The FSW process for AA1050-H12 and AA5754-H24 aluminum alloys was performed at weld speeds of 100, 300, and 500 mm/min. In all cases, the applied rotation speed was 600 rpm, and the tool plunge-depth (shoulder penetration) was 0.2 mm, and a tilt angle of 3° was applied.

The peak temperatures were measured on top surfaces of advancing side of weld joints using IR measuring device "Quicktemp 860-T3, 30…+900 °C". The plunge forces were recorded by the FSW machine control system.

**Table 1 – Chemical composition of the studied aluminum alloys.**

| Type | wt.% | | | | | | | | |
|---|---|---|---|---|---|---|---|---|---|
| | Si | Fe | Cu | Mn | Mg | Cr | Zn | Ti | Al |
| AA1050 | 0.08 | 0.27 | 0.02 | 0.01 | 0.01 | – | 0.02 | 0.02 | Rest |
| AA5754 | 0.4 | 0.4 | 0.1 | 0.5 | 2.6–3.2 | 0.3 | 0.2 | 0.15 | Rest |

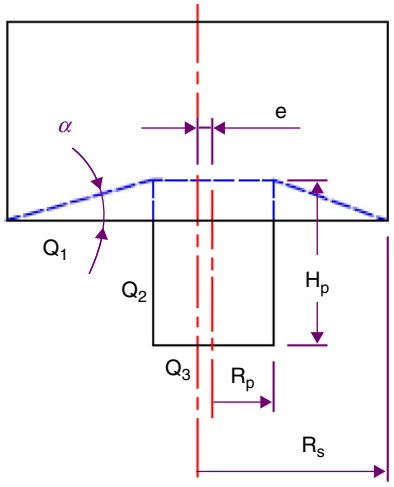


**Fig. 1 – Schematic drawing of FSW tool used showing the different heat generation regions.**

## 3. Analytical estimation of heat generation

Fig. 1 shows the simplified tool design with pin eccentricity and the three different regions of expected heat generation, where $Q_1$ is the heat generated by the concave shoulder, $Q_2$ is the heat generated by the pin side and $Q_3$ is the heat generated by the pin tip, hence the total heat generation:

$$Q_{total} = Q_1 + Q_2 + Q_3.$$

The following underlying assumptions were considered for the current analytical modeling.

- The analytical estimation based on a general assumption of uniform contact shear stress $\tau_{contact}$ was considered.
- The sliding condition of the shearing take place at the contact interface.
- Other mechanism of heat generation, such as deformation was not considered.
- In case of eccentric pin, two areas for contact interface must be considered, first, is the area of pin surface, and second, is the effective frictional area as can be seen in Fig. 2(c).

The contact surface between eccentric tool and workpiece given by position and orientation relative to rotation axis is shown in Fig. 2.

A simple tool design with concave shoulder surface, eccentric cylindrical pin surface and flat pin tip surface was used in the current analytical modeling, which is the modified version of the analytical model given by Schmidt et al. [17]. The concave shoulder surface is characterized by the concave angle $\alpha$, and eccentric cylindrical pin is characterized by the eccentricity distance $e$.

The expressions for each surface area orientation are different, but are based on the general equation for heat generation [17,18]:

$$dQ = \omega \cdot dM = \omega \cdot r \cdot dF = \omega \cdot r \cdot \tau_{contact} \cdot dA \quad (1)$$

### 3.1. Heat generation from the shoulder surface

In order to calculate the heat generation in the concave shoulder surface rotating around the tool center axis, an infinitesimal segment on that surface is considered. The infinitesimal segment area $dA_1 = r \cdot d\theta \cdot ds$ is exposed to a uniform contact shear stress $\tau_{contact}$. This segment contributes with an infinitesimal force of $dF = \tau_{contact} \cdot dA_1$ and torque of $dM = r \cdot dF$. The heat generation from this segment is:

$$dQ_1 = \omega \cdot r \cdot \tau_{contact} \cdot r \cdot d\theta \cdot ds \quad (2)$$

where $r$ is the distance from the considered area to the center of rotation, $\omega$ is the angular velocity, and $r \cdot d\theta$ and $ds$ are the segment dimensions, $ds = dr/\cos\alpha$. Integration of Eq. (2) over the concave shoulder area from $R_P$ to $R_s$ gives the shoulder heat generation, $Q_1$.

$$dQ_1 = \omega \cdot r^2 \cdot \tau_{contact} \cdot d\theta \cdot \frac{dr}{\cos\alpha}$$

$$Q_1 = \int_0^{2\pi} \int_{R_p}^{R_s} \omega \cdot r^2 \cdot \tau_{contact} \cdot d\theta \cdot \frac{dr}{\cos\alpha} \quad (3)$$

$$Q_1 = 2\pi \cdot \omega \cdot \tau_{contact} \cdot \frac{(R_s{}^3 - R_p{}^3)}{3\cos\alpha}$$

### 3.2. Heat generation from the pin side surface

The pin consists of eccentric cylindrical surface with a radius of $R_p$, eccentricity distance $e$ and pin height $H_p$. The heat generated from the pin side is given by Eq. (4) over the pin side area.

$$dQ_2 = \omega \cdot (r + e) \cdot \tau_{contact} \cdot (r + e) \cdot d\theta \cdot dz$$

$$Q_2 = \int_0^{2\pi} \int_0^{H_p} \omega \cdot (r + e)^2 \cdot \tau_{contact} \cdot d\theta \cdot dz = 2\pi \quad (4)$$

$$\cdot \omega \cdot \tau_{contact} \cdot (R_p + e)^2 \cdot H_p$$

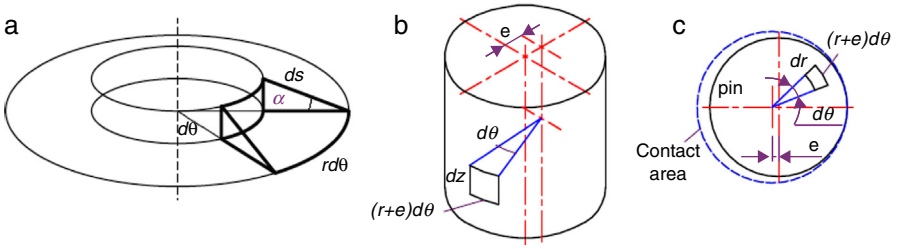


**Fig. 2 – Schematic drawing of surface orientations and infinitesimal segment areas: (a) concave shoulder, (b) pin side and (c) pin tip.**

### 3.3. *Heat generation from the pin tip surface*

The heat generated from the pin tip is given by Eq. (5) over the pin tip surface, assuming a flat pin tip gives pin tip heat generation, $Q_3$.

$$dQ_3 = \omega \cdot (r+e) \cdot \tau_{contact} \cdot (r+e) \cdot d\theta \cdot dr$$

$$Q_3 = \int_0^{2\pi}\int_0^{R_p} \omega \cdot (r+e)^2 \cdot \tau_{contact} \cdot d\theta \cdot dr \quad (5)$$

$$Q_3 = \frac{2}{3}\pi \cdot \omega \cdot \tau_{contact}\left((R_p+e)^3 - e^3\right)$$

From Eqs. (3)–(5), $Q_{Total}$ can be calculated as:

$$Q_{Total} = Q_1 + Q_2 + Q_3$$

$$Q_{Total} = \frac{2}{3}\pi \cdot \omega \cdot \tau_{contact}\left[\frac{({R_s}^3 - {R_p}^3)}{\cos\alpha} + 3H_p(R_p+e)^2 + \left((R_p+e)^3 - e^3\right)\right] \quad (6)$$

In the case of a flat shoulder ($\alpha = 0$) and pin without eccentricity ($e = 0$), the heat generation expression simplifies to:

$$Q_{Total} = \frac{2}{3}\pi \cdot \omega \cdot \tau_{contact}\left[R_s^3 + 3H_pR_p^2\right] \quad (7)$$

This correlates well with the results obtained by Schmidt et al. [17] and Gadakh et al. [18].

The shear stress estimates for a sliding condition is $\tau_{contact} = p \cdot \mu$ and pressure equals to the force divided by the shoulder area $p = F/\pi \cdot R_s^2$

The energy per unit length of the weld can be calculated by dividing Eq. (6) by the welding speed:

$$Q_{Energy/Length} = \frac{2\omega \cdot F \cdot \mu}{3v \cdot R_s^2}\left[\frac{(R_s^3 - R_p^3)}{\cos\alpha} + 3H_p(R_p+e)^2 + \left((R_p+e)^3 - e^3\right)\right] \quad (8)$$

The coefficient of friction ($\mu$) varies with temperature [18,19]. But in the present model for demonstration purpose it was considered as 0.5.

The effective energy per weld length ($Q_{Eff}$) [19] is defined as the energy per weld length multiplied by the transfer efficiency ($\beta$, ratio of the pin length $H_P$ to the work piece thickness $t$) and given by:

$$Q_{Eff} = \beta \cdot Q_{Energy/Length} = (H_p/t) \times Q_{Energy/Length} \quad (9)$$

For validation of the proposed model, an empirical relationship between the temperature ratio and the effective energy level has been developed based on the measured temperature during FSW of the studied aluminum alloys and the obtained energy level per unit length from the current analytical model. Fig. 3 plots the temperature ratio ($T_{Max}/T_s$) against the energy level per unit length data ($Q_{Eff}$) of FSWed AA1050-H12 and AA5754-H24. Linear regression curves have been added to the temperature ratio/energy level data to obtain an equation for each eccentricity case. It can be seen in Fig. 3 that six equations were derived from the linear regression curves. The first term in all the equations is almost the same, however, the second term in all the equations is slightly different. Accordingly it has been assumed that, the reason of this difference is due to the cooling rate effect that resulted from the ratio between the pin area and effective frictional area. In consequently, by compensating this effect in the linear regression equation the resulting empirical relationship between the temperature ratio and the effective energy level that can be applied in case of FSW of aluminum alloys using tool pin with eccentricity is found to be:

$$\frac{T_{Max}}{T_S} = 2 \times 10^{-4}Q_{Eff} + \frac{0.5 \times R_p^2}{(R_p+e)^2} \quad (10)$$

Eq. (10) describes a relationship between the temperature ratio and the effective energy level that is characteristic of different aluminum alloys that have approximately the same thermal diffusivity. Also this empirical relationship is similar to the empirical formula developed by Hamilton et al. [19].

## 4. Results and Discussion

The currently developed model for heat generation in FSW using eccentric tool pin has been used to calculate the energy per unit length and the peak temperature. Table 2 gives the welding process parameters, calculated energy per unit length ($Q_{Energy/length}$), calculated peak temperatures ($T_{max}$) compared with the measured temperatures during FSW of aluminum alloys AA1050-H12 and AA5754-H24 studied in this work.

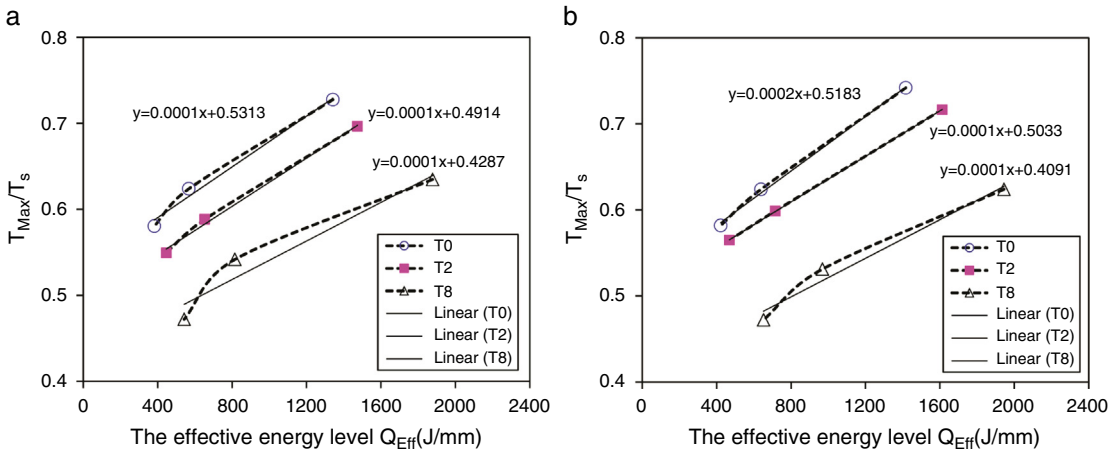


**Fig. 3 – Temperature ratio as a function of effective energy level with linear regression curve added: (a) FSWed AA1050-H12 and (b) AA5754-H2.**

**Table 2 – Welding process parameters of the Al alloys and calculated peak temperatures.**

| Alloy | RS (rpm) | WS (mm/min) | e (mm) | F (KN) | $Q_{Energy/length}$ (J/mm) | $T_{Measu.}$ (°C) | $T_{Max}$ (°C) |
|---|---|---|---|---|---|---|---|
| 1050-H12 | 600 | 100 | 0 | 9 | 1399 | 470 | 496.4 |
| | 600 | 300 | 0 | 11.2 | 568 | 403 | 396.4 |
| | 600 | 500 | 0 | 12.5 | 382 | 375 | 372.3 |
| | 600 | 100 | 0.2 | 9.6 | 1474 | 450 | 474.3 |
| | 600 | 300 | 0.2 | 12.5 | 653 | 380 | 368.2 |
| | 600 | 500 | 0.2 | 14.2 | 447 | 355 | 341.6 |
| | 600 | 100 | 0.8 | 11.2 | 1878 | 410 | 443.9 |
| | 600 | 300 | 0.8 | 14.3 | 815 | 360 | 306.6 |
| | 600 | 500 | 0.8 | 15.8 | 543 | 305 | 271.4 |
| 5754-H24 | 600 | 100 | 0 | 9.5 | 1476 | 440 | 464.5 |
| | 600 | 300 | 0 | 12.6 | 666 | 370 | 372.3 |
| | 600 | 500 | 0 | 13.8 | 439 | 345 | 346.5 |
| | 600 | 100 | 0.2 | 10.5 | 1670 | 425 | 451.8 |
| | 600 | 300 | 0.2 | 13.7 | 745 | 355 | 345.4 |
| | 600 | 500 | 0.2 | 14.9 | 488 | 335 | 316.2 |
| | 600 | 100 | 0.8 | 11.6 | 2026 | 370 | 415.4 |
| | 600 | 300 | 0.8 | 17 | 1010 | 315 | 299.7 |
| | 600 | 500 | 0.8 | 19 | 680 | 280 | 262.2 |

The calculated energy per unit length ($Q_{Energy/length}$) and calculated peak temperature are plotted against the tool pin eccentricity and compared with the measured peak temperature during FSW. Fig. 4(a) and (b) shows the variation of $Q_{Energy/length}$ with the tool pin eccentricity for friction stir welded FSWed AA1050-H12 and AA5754-H24, respectively. It can be observed that increasing the tool pin eccentricity has resulted in an increase of the energy per unit length at the same welding speed, which can be attributed to the increase of the rotation volume that required higher force as shown in Table 2. For example at 100 mm/min welding speed increasing the eccentricity from 0 to 0.8 mm has resulted in an increase of the energy per unit length from 1400 J/mm to 1800 J/mm in case of FSWed AA1050-H12. Also, a significant energy per unit length increase can be observed with decreasing the welding speed at all eccentricities used. For example, increasing welding speed from 100 mm/min to 500 mm/min has resulted in a decrease of energy per unit length from around 1400 J/mm to 380 J/mm.

Fig. 5(a) and (b) shows the variation of the calculated and measured peak temperatures with the FSW tool pin eccentricity for FSWed AA1050-H12 and AA5754-H24 aluminum alloys, respectively. Although the energy per unit length increases by increasing the eccentricity at each constant welding speed, both the calculated and measured peak temperatures decrease by increasing the pin eccentricity for the two studied aluminum alloys. This agreement between the measured and calculated peak temperatures is clarified in the next section by following the path of a point on the surface of the tool pin.

Fig. 6 shows the effect of tool pin eccentricity on the calculated peak temperature during FSW of AA1050-H12 and AA5754-H24. It can be seen in Fig. 6(a) and (b) that the peak temperature for the two aluminum alloys AA1050-H12 and AA5754-H24 decrease by increasing both the tool pin eccentricity and the welding speed. The effect of the welding speed is not surprising as by increasing the welding speed the heat input decrease as the number of revolution per mm is

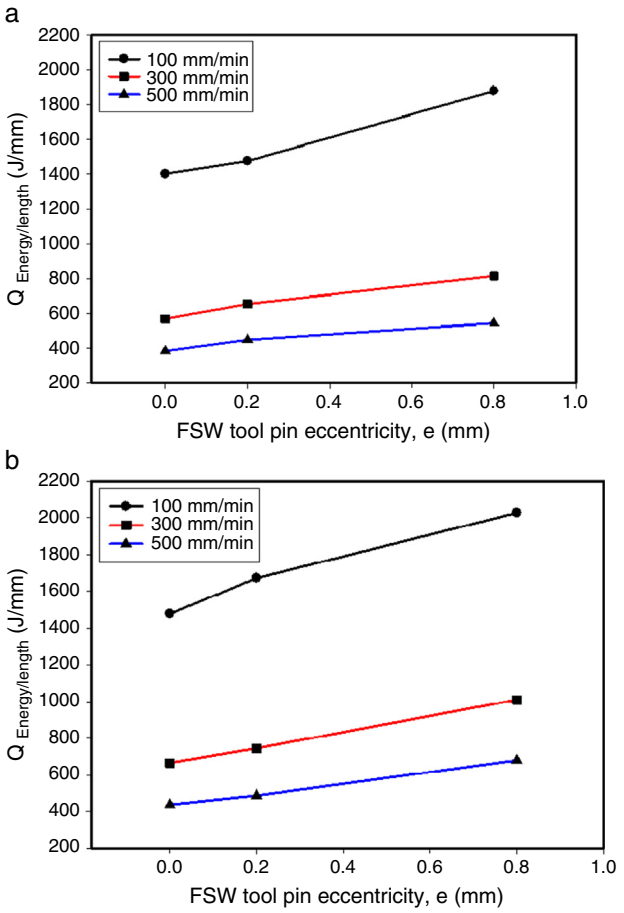


**Fig. 4 – The variation of $Q_{Energy/length}$ with the tool pin eccentricity for (a) FSWed AA1050-H12 and (b) AA5754-H2.**

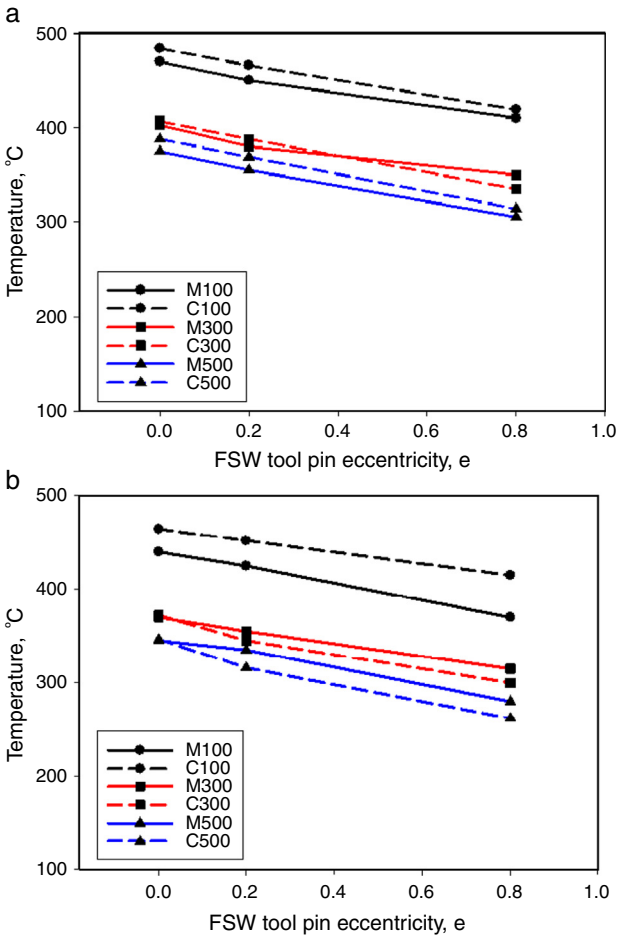


**Fig. 5 – Variation of calculated and measured peak temperature with the tool pin eccentricity for FSWed (a) AA1050-H12, (b) AA5754-H24 at different welding speeds of 100, 300 and 500 mm/min. M: stands for measured and C: stands for calculated.**

decreasing. However, the effect of the tool pin eccentricity can be attributed to the cooling rate effect in this region due to the long path with increasing the tool pin eccentricity.

This could be clarified further by following the path of a hypothetical point "a" on the pin surface produced by the tools with pin eccentricity of 0, 0.2, and 0.8 mm at welding speed of 500 mm/min, rotation speed of 600 rpm, and revolutionary pitch of 0.83 mm/rev (for one revolution), as shown in Fig. 7. The figure indicates clearly, that the path of point "a" produced by the tool with the pin eccentricity of 0.8 mm is longer than the corresponding paths produced by

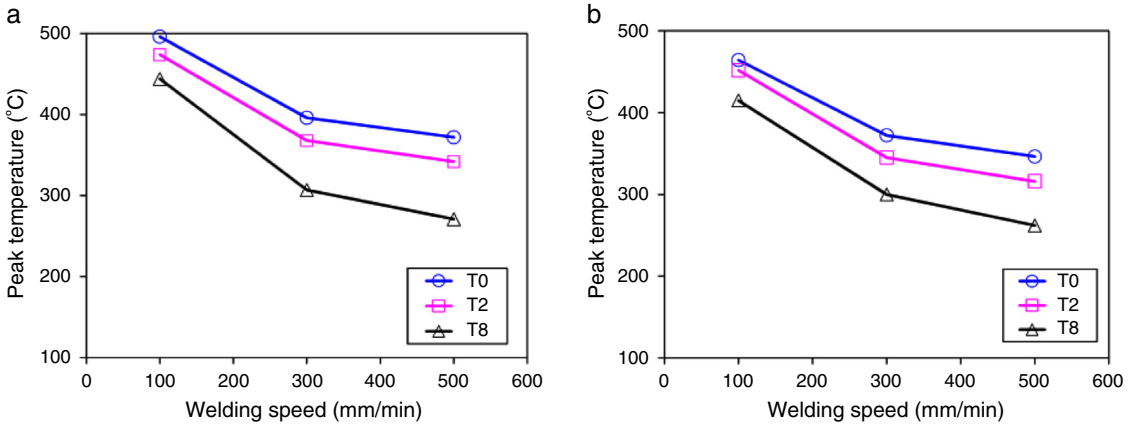


**Fig. 6 – Effect of tool pin eccentricity and welding speed on the calculated peak temperatures in FSW of (a) AA1050-H12 and (b) AA5754-H24.**

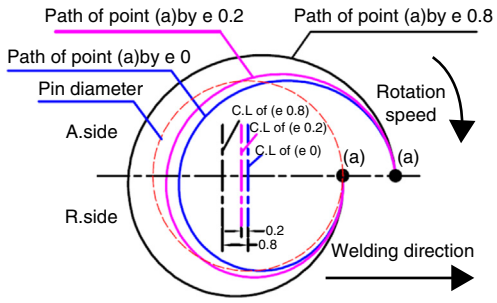


**Fig. 7 – Paths of point "a" on pin surface, at 500 mm/min welding speed, produced by tools with pin eccentricity (e) of 0, 0.2, and 0.8 mm.**

the other tools, and the effective frictional area by the tool with pin eccentricity of 0.8 mm is greater than the effective frictional area by the other tools. The heat generated by the tool with pin eccentricity of 0.8 mm is greater than the heat generated by the other tools. On the other hand, the cooling rate in weld joints welded by tool with pin eccentricity of 0.8 mm is higher than that in the weld joints welded by the other tools. This can explain the decrease of peak temperature with increase of tool pin eccentricity.

## 5. Conclusions

An analytical model for heat generation for eccentric cylindrical pin in FSW of Al alloys was developed. Based on present findings, it could be concluded that:

1. There is a good agreement between the generated heat energy and the associated maximum temperature by the proposed model and measured results.
2. With the proposed analytical model approach one can directly predict the peak temperature for respective tool pin eccentricity under given process conditions, which will be helpful for further predicting the mechanical properties for that Al alloy and hence elimination of post weld testing cost and time.
3. The developed model described in this study with modification in Eqs. (8)–(10) can be used to predict the peak temperature for different alloys and materials.

## Conflicts of interest

The authors declare no conflicts of interest.

## Acknowledgements

Authors would like to thank the Science and Technology Development Fund (STDF), Ministry of Scientific Research (Egypt) for funding this work with grant no 3926.

## REFERENCES

[1] Thomas WM, Nicholas ED, Needham JC, Murch MG, Templesmith P, Dawes CJ. International Patent Application No. PCT/GB92/02203 and GB Patent Application No. 9125978.8. U.S. Patent No. 5,460,317; 1991.
[2] Mishra RS, De PS, Kumar N. Friction stir welding and processing: science and engineering. Springer International; 2014.
[3] Su JQ, Nelson TW, Mishra RS, Mahoney M. Microstructural investigation of friction stir welded 7050-T651 aluminium. Acta Mater 2003;51:713–29.
[4] Jata KV, Sankaran KK, Ruschau J. Friction stir welding effects on microstructure and fatigue of aluminum alloy 7050-T7451. Metall Mater Trans A 2000;31:81–92.
[5] Nandan R, Roy TD, Bhadeshia H. Recent advances in friction stir welding process, weldment structure and properties. Prog Mater Sci 2008;53:980–5.
[6] Rhodes CG, Mahoney MW, Bingel WH. Effects of friction stir welding on microstructure of 7075 aluminium. Scr Mater 1997;36:69–75.
[7] Meilinger A, Török I. The importance of friction stir welding Tool. Prod Process Syst 2013;6:25–34.
[8] Rai R, De A, Bhadeshia H, Roy TD. Review: friction stir welding tools. Sci Technol Weld Join Forum 2011;16: 325–42.
[9] Fujii H, Cui L, Maeda M, Nogi K. Effect of tool shape on mechanical properties and microstructure of friction stir welded aluminum alloys. Mater Sci Eng A 2006;419:25–31.
[10] Thomas WM, Dolby RE. Friction stir welding developments. In: Proceedings of 6th international trends in welding research conference. 2002. p. 203–11.
[11] Elangovan K, Balasubramanian V. Influences of tool pin profile and tool shoulder diameter on the formation of friction stir processing zone in AA6061 aluminum alloy. Mater Des 2008;29:362–73.
[12] Thomas WM, Nicholas ED. Friction stir welding for the transportation industries. Mater Des 1997;18:269–73.
[13] Gratecap F, Girard M, Marya S, Racineux G. Exploring material flow in friction stir welding: Tool eccentricity and formation of banded structures. Int J Mater Form 2011;5:99–107.
[14] Tingey C, Galloway A, Toumpis A, Cater S. Effect of tool centreline deviation on mechanical properties of friction stir welded DH36 steel. Mater Des 2015;65:896–906.
[15] Yuqing M, Liming K, Fencheng L, Qiang L, Chunping H, Li X. Effect of tool pin eccentricity on microstructure and mechanical properties in friction stir welded 7075 aluminum alloy thick plate. Mater Des 2014;62:334–43.
[16] Khandkar MZH, Khan JA, Reynolds AP. Prediction to temperature distribution and thermal history during friction stir welding: input torque based model. Sci Technol Weld J 2003;8:165–74.
[17] Schmidt H, Hattel J, Wert J. An analytical model for the heat generation in friction stir welding. Model Simul Mater Sci Eng 2004;12:143–57.
[18] Gadakh VS, Kumar Adepu K. Heat generation model for taper cylindrical pin profile in FSW. Mater Res Technol J 2013;2(4):370–5.
[19] Hamilton C, Dymek S, Sommers A. A thermal model of friction stir welding in aluminum alloys. Int J Mach Tools Manuf 2008;48:1120–30.